

Reflective Semiconductor Optical Amplifier Modulator Dynamic Model

M. J. Connelly

Optical Communications Research Group, Dept. Electronic and Computer Engineering, University of Limerick, Limerick, Ireland. E-mail: michael.connelly@ul.ie.

Abstract- A dynamic model of a bulk reflective SOA is described. The model includes spontaneous emission and uses full bandstructure based calculations of the active material gain coefficients. The model is used to simulate the use of an RSOA to modulate an input CW lightwave at multi Gb/s data rates using bias current modulation. Simulated eye diagrams show good agreement with experiment.

I. INTRODUCTION

* Reflective semiconductor optical amplifiers (RSOAs) have shown promise for applications in WDM optical networks including as basic amplifiers and also as optical modulators. In the latter application an input CW lightwave is modulated by the amplifier using bias current modulation. There is a need for models that can be used to predict RSOA dynamics and in particular the effect of such dynamics when the RSOA is used to modulate a CW lightwave using bias current modulation at multi Gb/s data rates.

In this paper we extend our prior work on traveling-wave and reflective SOAs [1-4], to develop an RSOA dynamic model that includes facet reflections and amplified spontaneous emission (ASE). A full bandstructure active material model is used to determine the wavelength and carrier density dependency of the material gain and additive spontaneous emission. The model and includes a full geometrical description of the amplifier waveguide, including the input taper and the position dependency of the TE/TM confinement factors. The amplified signal and ASE are described by travelling-wave equations and numerically solved in conjunction with a carrier density rate equation. The model uses material and geometric parameters for a commercially available tensile-strained bulk RSOA (manufactured by Kamelian), whose active waveguide is shown in Fig. 1. The versatility of the model is shown by simulations that are used to predict the modulated CW signal eye-diagrams.

II. THEORY, NUMERICAL MODEL AND SIMULATIONS

SOA dynamics are governed by the interaction between the injected signal, amplified spontaneous emission and the carrier density. In the model the relevant dynamics occur on time scales much greater than the SOA transit time (approximately 8.5 ps) so the signal and ASE can be assumed to propagate

instantaneously across the SOA length. The active region carrier density n rate equation is

$$\frac{dn}{dt} = \frac{\eta I(t)}{eV} - R(n) - \frac{\Gamma_{s,p}}{dW(z)} g_{m,TE/TM} I_{s,TE/TM}^{\pm} - \frac{1}{dW(z)} \sum_{TE,TM} \sum_{k=1}^M \Gamma_{TE/TM}(z) g_{m,TE/TM,k} N_{TE/TM,k}^{\pm}(z) \quad (1)$$

The terms on the RHS of (1) are the current pump, spontaneous and Auger recombination, and carrier depletion due to the amplified signal $I_{s,TE/TM}^{\pm}$ and ASE $N_{TE/TM,k}^{\pm}$ (k-th spectral slice) photon rates. g_m is the active region material gain, whose dependency on energy and carrier density is determined using a full bandstructure model [4]. The model uses $M = 264$ spectral slices spanning a wavelength range of 300 nm centered at 1550 nm. The forward and backward propagating signal and spontaneous emission rates are determined by the traveling-wave equations

$$\frac{dI_{s,TE/TM}^{\pm}}{dz} = \pm g_{TE/TM} I_{s,TE/TM}^{\pm} \quad (2)$$

$$\frac{dN_{TE/TM,k}^{\pm}}{dz} = \pm g_{TE/TM,k} N_{TE/TM,k}^{\pm} \pm R_{sp,TE/TM,k} \quad (3)$$

, taking into account the boundary conditions at the reflecting facet. R_{sp} accounts for additive spontaneous emission and determined using the full bandstructure material model [4]. $g_{TE/TM}$ is the net gain coefficient that includes the optical confinement factor and the scattering loss. (1) is solved using finite differences. 128 time steps were used per modulation period. The maximum time step used is much less than the minimum value of the carrier lifetime encountered (typically > 100 ps), which ensures algorithm stability. At each time step the associated signal and ASE spatial distributions are obtained using finite difference solutions of (2) and (3), with 64 spatial steps. In the simulations we consider NRA data, with rise and fall times equal to one fifth of the bit-rate. The optical receiver comprises an optical filter of 0.8 nm bandwidth, an ideal photodetector (assuming a 50 Ω load), and a Gaussian low-pass filter having a time-bandwidth product of 0.75. The receiver electrical noise, comprising thermal noise, signal-spontaneous and spontaneous-spontaneous beat noise are modeled as white noise and then electrically filtered.

* This research was supported by Science Foundation Ireland Investigator Grant 09/IN.1/I2641.

In order to verify the accuracy of the model, the RSOA current was modulated, using a 2.5 GHz bandwidth current driver, by 1.25 Gb/s 2^9-1 PRBS NRZ data, where a '0' bit corresponds to a current of 10 mA and '1' bit to 100 mA. The RSOA small-signal gain at these currents -12 dB is and 17 dB respectively. The input CW lightwave power was -10 dBm at a wavelength of 1550 nm. Good agreement between simulated and experimental RSOA output eye diagrams was obtained as shown in Fig. 2. Pattern effects are evident because of the finite carrier recovery lifetime. Typical carrier density dynamics are shown in Fig. 3 along with the modulation current and output optical power. At 1.25 Gb/s pattern effects do give rise to some jitter but are not particularly serious. Some overshoot occurs on the transition from a '1' to a '0'. However as the data rate increases, pattern effects become more serious as shown in the simulations of Fig. 4 for 2.5 and 5 Gb/s data and in the latter case, the modulator performance is very poor.

III. CONCLUSION

A dynamic model of an RSOA has been described. The model can be used to determine the performance of an RSOA modulator and shows good agreement with experimental eye diagrams for NRZ data. Future work will investigate the use of more advanced modulation formats including RF current modulation.

REFERENCES

- [1] M. J. Connelly, "Reflective Semiconductor Optical Amplifier Pulse Propagation Model," *IEEE Photon Tech. Lett.*, vol. 24, no. 2, pp. 95-97, 2012.
- [2] M. J. Connelly, "Wideband dynamic numerical model of a tapered buried ridge stripe semiconductor optical amplifier gate," *Proc. IEE Circuits Devices Syst.*, 2002, vol. 149, pp. 173-178.
- [3] M. J. Connelly, "Wideband Semiconductor Optical Amplifier Steady-State Numerical Model," *IEEE J. Quantum Electron.*, vol., 37, no. 3, pp. 439-447, 2001.
- [4] M. J. Connelly, "Wide-band Steady-State Numerical Model and Parameter Extraction of a Tensile-Strained Bulk Semiconductor Optical Amplifier," *IEEE J. Quantum Electron.*, vol., 43, no. 1, pp. 47-56, 2007.

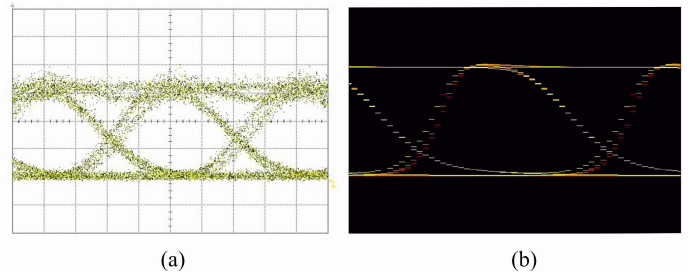


Fig. 2. (a) Experimental and (b) simulated eye diagrams for 1.25 Gb/s data.

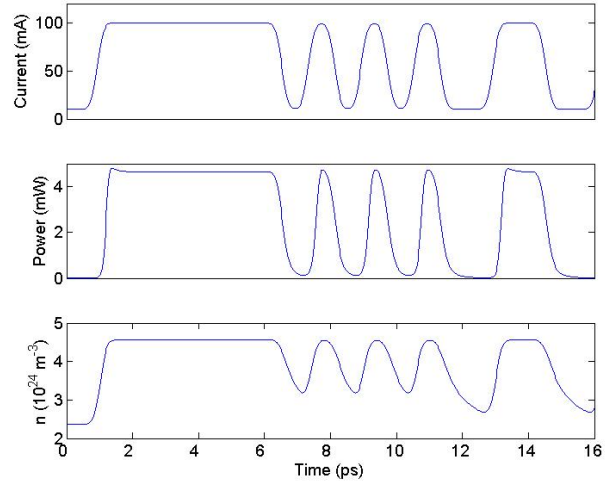


Fig. 3. Modulation current, output optical power and spatially averaged carrier density dynamics for 1.25 Gb/s data.

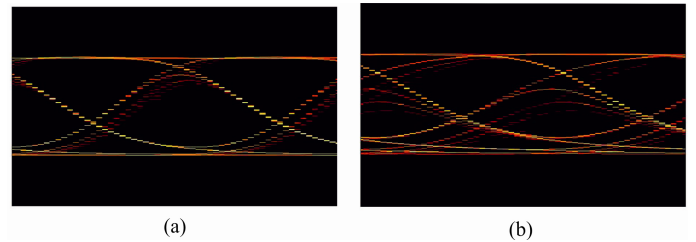


Fig. 4. (a) RSOA modulator simulated output eye diagrams for (a) 2.5 and (b) 5 Gb/s 2^9-1 PRBS data.

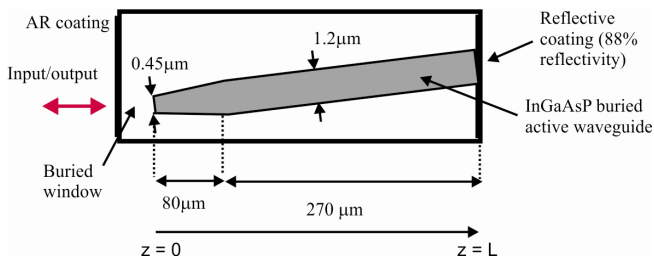


Fig. 1. Top view of the RSOA active waveguide.